Direct evidence for self-annihilation of antiphase domains in GaAs/Si heterostructures

O. Ueda
Fujitsu Laboratories Ltd., 10-1 Morinosato-Wakamiya, Atsugi 243-01, Japan

T. Soga, T. Jimbo, and M. Umeno
Department of Electrical and Computer Engineering, Nagoya Institute of Technology, Gokiso-cho, Showa-ku, Nagoya 466, Japan

(Received 22 November 1988; accepted for publication 18 May 1989)

The nature and behavior of antiphase boundaries in GaAs/Si heterostructures using GaP, GaP/GaAsP, and GaAsP/GaAs strained-layer superlattices as intermediate layers have been studied by transmission electron microscopy. The antiphase domains are found to be very complicated three-dimensional polygons consisting of several subboundaries in different orientations. Self-annihilation of antiphase domains during crystal growth of GaAs on (001) 0.4° off or (001) 2° off Si substrates is directly observed for the first time through plan-view and cross-sectional observations. Based on these findings, a mechanism of annihilation of these domains is presented.

To date, much effort has been put into the investigation of defects generated in highly mismatched heteroepitaxy such as GaAs/Si(Ge),[1–5] GaP/Si,[6] etc. Current major issues in these systems are (1) introduction of a high density of defects, mostly threading dislocations propagating from the interface between the epitaxial layer and the substrate and those generated from the surface by thermal stress, and (2) accumulation of internal stress due to the difference in thermal expansion coefficients between the epitaxial layer and the substrate, e.g., GaAs and Si, during the cooling process after growth. The current best data for dislocation density evaluated by plan-view transmission electron microscopic (TEM) observation are known to be in the low 10^6 cm^{-2}, achieved by the combination of standard low-high two-step growth technique and thermal annealing during growth,[7] or using strained-layer superlattice (SLS) as intermediate buffer layers.[8,9] However, for the second issue, the situation has not been drastically changed yet.[10]

The problem of antiphase domains (APDs)[11] has received considerable attention in the past; it is now recognized that they can be practically controlled by using (001) more than 2° off Si as a substrate.[12] However, the exact nature and mechanism for their generation (and annihilation, if any) cannot be fully understood yet. Etch pitting with molten KOH is the most commonly used method for revealing APDs[13]; one can identify antiphase boundaries (APBs) by the presence of two kinds of etch pits elongating in equivalent ⟨110⟩ orientations on both sides of the boundary. Since the typical diameter of these etch pits is in the 1–3 μm range, submicron-size APDs are not detected by this method. TEM is the most powerful method for microscopic identification of APDs. At present, two unique techniques can be employed for surveying APDs. One is the convergent beam electron diffraction (CBED) approach, which was originally demonstrated by Taftϕ and Spence.[14] The other is the $\pm$002 dark field imaging technique proposed by Kuan.[15] The latter method is a very simple one; thus, we have also employed this method in our experiments. The technique enables us to produce distinct dark and bright contrast on both sides of the APB, although the contrast is strongly related to the foil thickness. Additionally, we have found that standard bright field imaging under a two-beam diffraction condition can also reveal the existence of large-diameter APDs.

In this letter, we describe for the first time a detailed structural investigation of APDs by TEM and present direct evidence for their self-annihilation.

Crystals were grown by metalorganic chemical vapor deposition (MOCVD). The heterostructure consists of a GaP buffer layer (0.1 μm), followed by SLSs of GaP/$GaAs_{0.5}P_{0.5}$ and $GaAs_{0.5}P_{0.5}$/GaAs (five periods for each SLS and 20 nm for each layer), and finally a thick GaAs layer (4 μm). The growth temperatures for the GaP, SLSs, and GaAs were 900, 750, and 750 °C, respectively. TMG, AsH_3, and PH_3 were used as reactants (the detailed growth procedure is described elsewhere).[16,17] Two types of heterostructures were examined. Type I was grown on (001) 0.4° off toward [110] Si substrate and type II on (001) 2° off toward [110] substrate.

Both plan-view and cross-section TEM observations were carried out; in both cases, specimen preparation was done by ion thinning. TEM observations were carried out in an Akashi ultrahigh-resolution analytical electron microscope EM-002B operated at 200 kV.

First of all, plan-view and cross-section TEM observations were performed for type I structures. From plan-view observations we find uniformly distributed domain-like regions of the type shown in Fig. 1. It is concluded that these regions correspond to APDs for the following reasons. (1) No extra spots associated with small-angle tilt boundaries are found in the electron diffraction pattern from the area containing the domain-like regions. (2) Although some part of the boundary has fringe contrast, this contrast is not due to a stacking fault since it does not vanish under any reflections in the (001) pole, and it is not asymmetric in the dark field image. (3) In the electron diffraction pattern from areas including the domain-like regions in the (110) and ($1\bar{1}0$) cross sections, no twin-related spots are observed. (4)

 0003-6951/89/310445-03$01.00

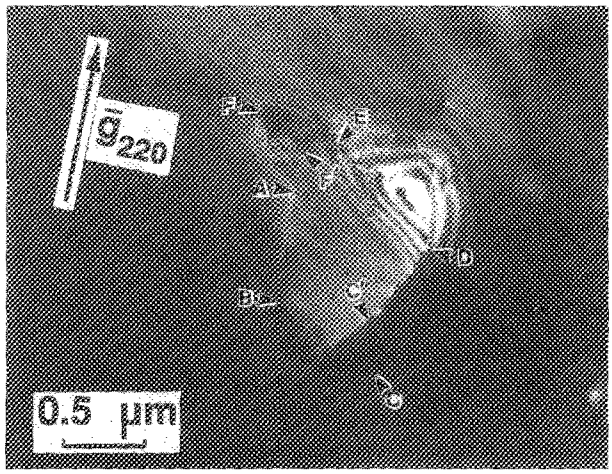

FIG. 1. Plan-view bright field TEM image illustrating a typical antiphase domain in the GaAs top layer of the GaAs/SLSs/GaP/Si heterostructure grown on a (001) 0.4° off Si substrate, obtained from the 220 reflection.

In cross-section observations, the contrast of the domain in a dark field image is reversed when the reflection vector is changed from 002 to $00\bar{2}$ as illustrated in Fig. 2 (details for Fig. 2 are described later).

The domain size is found to be in the range 0.5–2.0 μm; thus, the etch pitting technique would not be expected to detect these small APDs, since etch pits are larger than 1 μm in most cases. Each APD has a different geometry; they are found to be three-dimensional extended polygon-shaped structures consisting of many different subboundaries. These subboundaries are classified into two types: those nearly normal to the (001) plane and those inclined to the (001) plane. In Fig. 1, since the subboundaries denoted by *A-B* and *D-E* do not display fringe contrast, they are expected to be normal to the (001) plane. From the directions of their elongation, they are possibly (110) and (100) oriented boundaries, respectively. From plan-view observations it is found that most of the APBs normal to the (001) plane are {110} or {100} boundaries. The other boundaries denoted by *B-C-D-C'-B* and *A-F'-E-F* are curved and exhibit fringe contrast. This may be due to the phase shift of the electron beam when the electrons re-enter from the matrix crystal to the APD. Thus, they are inclined to the (001) plane and are perhaps a mixture of tilted APBs indexed as (11*n*) [such as (111) and (112)] and (10*n*) [such as (101) and (102)].

In each boundary, a number of dislocations can be seen. In this case, these boundary dislocations are invisible under the reflection of 400 or 040. Since most of the APBs are not lying on the {111} plane, these boundary dislocations cannot glide at all. Also in the case where stacking faults and microtwins are generated in the APD, they cannot be expected to extend to the region outside the APD, since there is a clear difference in the atomic arrangement between the APD and matrix crystal.

From steroscopic observations it is found that the circuit denoted by *A-B-C-D-E-F-A* in Fig. 1 is lying below the top surface and that the circuit denoted by *A-B-C'-D-E-F'-A* is lying on the top surface. This finding strongly suggests that the domain size becomes smaller during the sequence of crystal growth, with self-annihilation occurring as a final stage.

Surprisingly, we have discovered direct evidence for this speculation in the cross-section TEM image shown in Fig. 2. Figures 2(a) and 2(b) are dark field images taken by weak 002 and $00\bar{2}$ reflections obtained from the (110) cross-section specimen of type I. A high density of defects (mostly dislocations) is present in both the GaP buffer layer and the SLSs, since the crystal is grown on (001) 0.4° off Si. In both figures, a domain extending from the interface between the Si substrate and the GaP buffer layer into the GaAs layer is observed (see the domain denoted by APD), although the contrast of the boundary in the region below the SLSs is not clear due to the high defect density. It should be noted that in Fig. 2(a) the domain contrast is bright whereas that of the matrix region is dark. On the other hand, the opposite result is obtained in Fig. 2(b). Since due to the lack of twofold axes along the ⟨110⟩ direction in the zinc blende structure, the amplitudes of the 002 and the $00\bar{2}$ reflections are not equal for most crystal thicknesses, the image intensities from both sides of the APB must be different except for certain foil thickness. Based on this consideration, the domain observed in Figs. 2(a) and 2(b) is identified to be an APD similar to that shown in Fig. 1. As can be seen in these micrographs, the APD annihilates in the intermediate layer of GaAs by changing the orientation of subboundaries from normal to (001) to higher index planes (see also the region denoted by arrows).

On the basis of these results, the following scenarios are derived for the self-annihilation mechanism of APDs during crystal growth:

(a) At the initial stage of crystal growth, three-dimensional island growth proceeds at the step edges. By the coalescence of islands with two different phases (i.e., matrix phase and antiphase), APDs are structurally introduced.

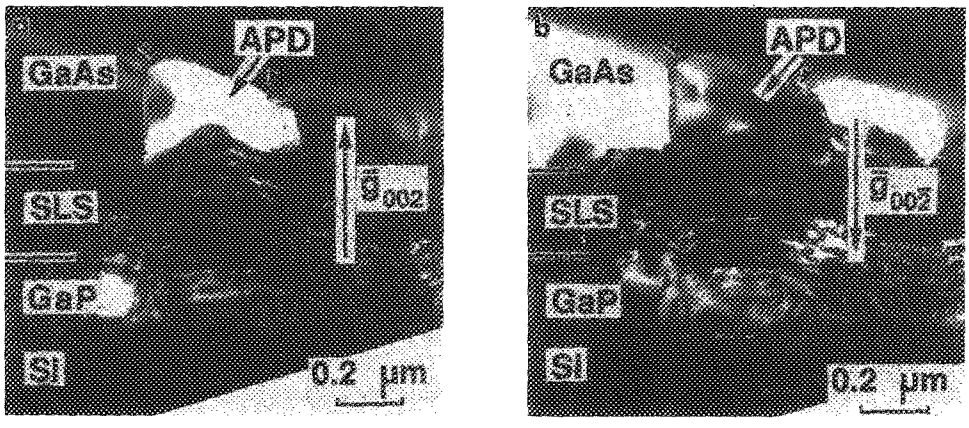

FIG. 2. Cross-section dark field images illustrating the GaAs/SLSs/GaP/Si heterostructure obtained by the weak 002 and $00\bar{2}$ reflections. An antiphase domain (see the region denoted by APD) self-annihilating in the intermediate layer of GaAs is observed. (a) $\vec{g} = 002$; (b) $\vec{g} = 00\bar{2}$.

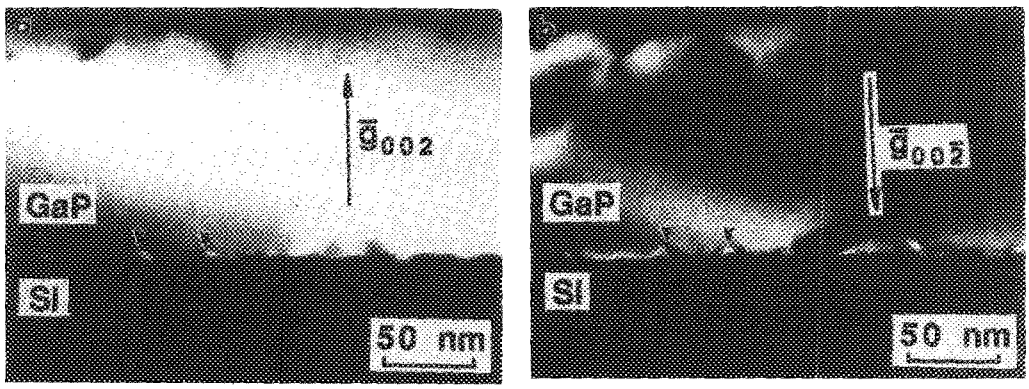

FIG. 3. Cross-section dark field images illustrating the GaP/Si interface in the GaAs/SLSs/GaP/Si heterostructure grown on a (001) 2° off Si substrate, obtained by the weak 002 and 00$\bar{2}$ reflections. (a) $\bar{g} = 002$; (b) $\bar{g} = 00\bar{2}$.

The APDs may be originally columnar shaped, consisting of several subboundaries predominantly nearly normal to the (001) plane such as (110) and (100). Alternately, the subboundaries may be inclined to the (001) plane from an early stage of crystal growth, in which case step (c) takes place immediately.

(b) When the thickness of the APD reaches a critical value, these subboundaries change their orientation to the higher index plane inclined to the (001) plane [such as the (112) plane which is the orientation with lowest energy[18]] so as to minimize the total energy in the system.

(c) By the coalescence of APBs with opposite orientation, the APD finally annihilates itself at the intermediate layer.

At this moment, the reason for the existence of, e.g., (100) APBs, which have a higher generation energy than (110) and (112) APBs, at the initial stage of crystal growth is not clear.

Next, type II samples are examined. From plan-view observations, APDs which are similar to those shown in Figs. 1 and 2 are not detected in the surface region of the GaAs layer. Figures 3(a) and 3(b) are 002 and 00$\bar{2}$ dark field TEM images from the (110) cross section, illustrating the interface between the GaP buffer layer and the Si substrate. Hillock-like microdomains are observed in the GaP buffer layer near the interface (see arrows). The variation of the diffraction contrast of these microdomains is very similar to that of the APDs shown in Figs. 1 and 2. Moreover, in this case, conditions (1)–(3) above are satisfied. Therefore, it is concluded that they are also APDs, although very small, with diameters of 10–20 nm. Provided that there are a certain number of monolayer steps on the surface of a (001) 2° off Si substrate (there is still controversy about the existence of double-layer steps on the vicinal surface of Si), the frequent presence of APDs is well explained by the average spacing between monolayer steps, i.e., approximately 4 nm. Regarding the self-annihilation of APDs at the initial stage of crystal growth on tilted substrates, there have been two competing models, one by Pukite and Cohen[19,20] and the other by Kawabe *et al.*[21,22] Although the subboundaries of the hillock-like APDs shown in Fig. 3 are lying nearly on the {112} planes, our findings described above strongly support the latter model.[21,22]

A more detailed analysis on the structure and distribution of APDs in this heterostructure and a TEM study of APDs in a GaAs/Si heterostructure grown by a standard two-step MOCVD technique will be reported in another paper.

In conclusion, we have investigated the nature and behavior of APBs in GaAs/Si heterostructures with GaP, GaP/GaAsP, and GaAsP/GaAs SLSs as intermediate buffer layers grown by MOCVD via TEM. It has been found that the size of the APDs depends on the offset angle of the Si substrate. The APDs observed are very complicated three-dimensional polygons and consist of several subboundaries in different orientations. We have also discovered the self-annihilation of APDs at the intermediate layer as a result of a change in the orientations of the subboundaries. Finally, a simple model for the generation of APDs has been presented.

The authors express their gratitude to O. Otsuki for his continuing encouragement throughout this work. They also thank A. Hobbs for valuable discussions.

[1]R. Fischer, H. Morkoç, D. A. Neumann, H. Zabel, C. Choi, N. Otsuka, M. Longbone, and L. P. Erickson, J. Appl. Phys. **60**, 1640 (1986).
[2]J. H. Mazur, J. Washburn, T. Henderson, J. Klem, W. T. Masselink, R. Fischer, and H. Morkoç, Mater. Res. Soc. Symp. Proc. **37**, 103 (1985).
[3]R. Hull, S. J. Rosner, S. M. Koch, and J. S. Harris, Jr., Appl. Phys. Lett. **49**, 1714 (1986).
[4]K. Ishida, M. Akiyama, and S. Nishi, Jpn. J. Appl. Phys. **26**, L163 (1987).
[5]N. Otsuka, C. Choi, Y. Nakamura, S. Nagakura, R. Fischer, C. K. Peng, and H. Morkoç, Appl. Phys. Lett. **49**, 277 (1986).
[6]M. M. Al-Jassim, A. E. Blakeslee, K. M. Jones, and S. E. Asher, Inst. Phys. Conf. Ser. **87**, 99 (1987).
[7]M. Yamaguchi, A. Yamamoto, M. Tachikawa, Y. Itoh, and M. Sugo, Appl. Phys. Lett. **53**, 2293 (1988).
[8]N. Hayafuji, S. Ochi, M. Miyashita, M. Tsugami, T. Murotani, and A. Kawagishi, J. Cryst. Growth **93**, 494 (1988).
[9]O. Ueda, T. Soga, T. Jimbo, and M. Umeno, to be presented at the 9th Int. Conf. Crystal Growth, Sendai, Japan, 1989 (to be published in J. Cryst. Growth).
[10]K. Ishida, M. Akiyama, and S. Nishi, Jpn. J. Appl. Phys. **26**, L530 (1987).
[11]H. Kroemer, J. Cryst. Growth **81**, 193 (1987).
[12]T. Ueda, S. Nishi, Y. Kawarada, M. Akiyama, and K. Kaminishi, Jpn. J. Appl. Phys. **26**, L530 (1987)
[13]K. Mizuguchi, N. Hayafuji, S. Ochi, T. Murotani, and K. Fujikawa, J. Cryst. Growth **77**, 509 (1986).
[14]J. Taftø and J. C. H. Spence, J. Appl. Cryst. **15**, 60 (1982).
[15]T. S. Kuan, J. Appl. Phys. **54**, 4408 (1983).
[16]T. Soga, T. Imori, M. Umeno, and S. Hattori, Jpn. J. Appl. Phys. **26**, L536 (1987).
[17]T. Soga, Y. Kohama, K. Uchida, M. Tajima, T. Jimbo, and M. Umeno, J. Cryst. Growth **93**, 499 (1988).
[18]P. M. Petroff, J. Vac. Sci. Technol. B **4**, 874 (1986).
[19]P. R. Pukite and P. I. Cohen, J. Cryst. Growth **81**, 193 (1987).
[20]P. R. Pukite and P. I. Cohen, Appl. Phys. Lett. **50**, 1739 (1987).
[21]K. Kawabe, T. Ueda, and H. Takasugi, Jpn. J. Appl. Phys. **26**, L114 (1987).
[22]K. Kawabe and T. Ueda, Jpn. J. Appl. Phys. **26**, L944 (1987).